A measurement of two-photon exchange in unpolarized elastic positron–proton and electron–proton scattering

J. Arrington (Spokesperson), T. Hague, S. Li, E. Sichtermann
Lawrence Berkeley National Laboratory, Berkeley, CA

M. Nycz (Spokesperson)
University of Virginia, Charlottesville, VA

E. Long, D. Ruth, S. N. Santiesteban (Spokesperson), K. Slifer, A. Zec
University of New Hampshrie, Durham, NH

M. Yurov (Spokesperson)
Mississippi State University, Starkville, MS

(Dated: May 16, 2023)

Abstract

Rosenbluth extractions of the proton form factors have limited sensitivity to the charge form factor $G_E(Q^2)$ at large Q^2 values (above a few GeV^2), as the cross section is dominated by the magnetic form factor, $G_M(Q^2)$. Polarization transfer measurements are directly sensitive to the ratio G_E/G_M, and were expected to provide greater sensitivity to G_E at large Q^2 values. However, Jefferson Lab measurements of G_E/G_M using polarization degrees of freedom showed that the ratio G_E/G_M dropped almost linearly with Q^2, while Rosenbluth separations show a constant value for G_E/G_M, albeit with lower precision. Based on a significant amount of advancement in theory and several new experimental studies, it is now generally believed that two-photon exchange (TPE) contributions explain this discrepancy. However, while comparisons of positron–proton and electron–proton scattering can isolate TPE contributions, existing data are limited to lower Q^2 values, where the discrepancy between the techniques is not so clear and experiments indicate only small TPE contributions.

We propose a series of high precision measurements of elastic positron–proton (and electron–proton) scattering over a wide kinematic range, $1.4 \leq Q^2 \leq 5.5$ GeV^2 to make a precise extraction of the ratio of the proton electric to magnetic form factors. We use the 'Super-Rosenbluth' technique, which involves detecting the struck proton rather than the scattered electron. The Super-Rosenbluth has been shown to allow for a much more precise extraction of the Rosenbluth slope, and thus G_E/G_M if we neglect two-photon exchange (TPE). Because two-photon exchange contributions are believed to modify the Rosenbluth slope, but have much smaller impact on polarization measurements, a comparison of either the positron or electron Rosenbluth G_E/G_M to that from polarization provides strong constraints on TPE contributions. The direct comparison of positron and electron Super-Rosenbluth separations will double the sensitivity to TPE corrections while, for the first time, directly test the hypothesis that the observed discrepancy at high Q^2 is explained by TPE contributions.

I. INTRODUCTION

The radial distribution of the charge and magnetization inside the proton are studied largely by the knowledge of the electric and magnetic form factors [1–3], G_E and G_M. Over several decades, several experiments have extracted the proton form factors via the Rosenbluth separation technique by making measurements of the angular dependence of the unpolarized proton-electron scattering cross section. The reduced cross section in the one-photon exchange (OPE) approximation goes as $\tau G_M^2 + \varepsilon G_E^2$, where $\tau = Q^2/(4M_p^2)$ and ε is the virtual photon polarization parameter which, at fixed momentum transfer Q^2, depends on the electron scattering angle. At large Q^2 values, τG_M^2 is much larger than εG_E^2, meaning that G_E contributes only a small ε dependence to the cross section, limiting the precision of G_E extractions [4–7]. Previous measurements found $\mu_p G_E/G_M \approx 1$ over a wide range in Q^2, but with limited precision at larger Q^2 values, where G_M dominates the cross section.

At JLab, experiments measuring the recoil polarization in elastic $\vec{e}$-p scattering were used to improve the extraction of G_E at large Q^2. These measurements are directly sensitive to G_E/G_M, providing significantly better sensitivity to G_E when combined with Rosenbluth measurements. Unexpectedly, the polarization measurements showed a linear fall-off of the $\mu_p G_E/G_M$ ratio with Q^2 [8–10], inconsistent with the observation of approximate form factor scaling from Rosenbluth separations [11]. The difference between these two measurements has been of studied extensively and the discrepancy is generally attributed to two-photon exchange [12–14], and comparisons of the Rosenbluth and polarization results have been used to extract the contribution of TPE under a set of common assumptions [7, 15–17].

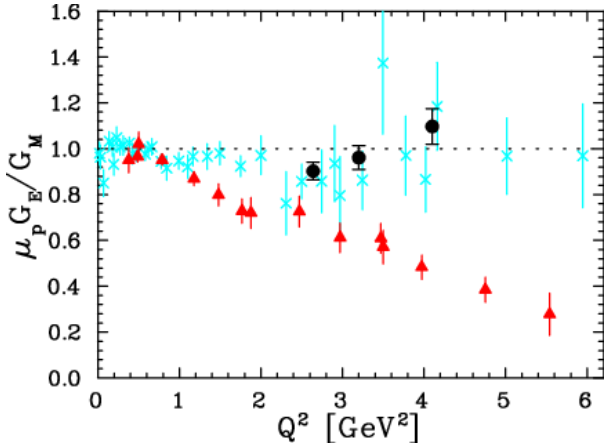

FIG. 1. Ratio R = $\mu_p G_E/G_M$ as extracted using Rosenbluth separation [15] (cyan crosses), polarization transfer measurements [9, 10, 18, 19] (red triangles), and "Super-Rosenbluth" measurements [20] (black circles); figure taken from [21].

The difference between Rosenbluth and polarization transfer [8, 22] measurements is illustrated in Figure 1, which shows a collection of G_E/G_M extractions using both techniques. Note that the black points are from the first "Super-Rosenbluth" measurement performed in Hall A (JLab E01-001) [20]. This is a modified version of a conventional Rosenbluth technique that uses proton detection rather than electron detection to minimize the ε-dependent

systematic uncertainties, thus giving a much better precision on the extraction of the ratio G_E/G_M, at the cost of larger absolute uncertainties on G_E and G_M.

TPE contributions are expected to be small, having only few-percent level contributions to the cross section and polarization transfer data. While these contribution have minimal impact on the extraction of G_E/G_M for polarization data, Figure 2 illustrates how small TPE contributions can yield a significant difference between Rosenbluth and polarization results if they have the correct ε dependence. At large Q^2 values, the ε dependence coming from G_E is small, since the G_E term is suppressed relative to G_M by a factor of $1/Q^2$, and the ratio G_E/G_M (as determined from polarization measurement) decreases with Q^2. As seen in Fig. 2, above $Q^2 \approx 2.5$ GeV^2, the polarization transfer data show that the cross section should have an ε dependence below 5%, meaning that TPE corrections at the few percent level can have a significant impact.

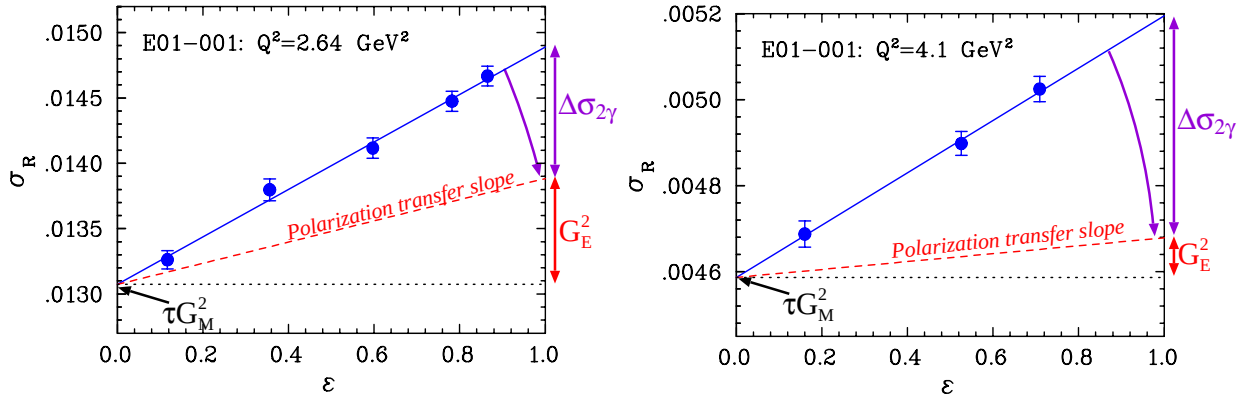

FIG. 2. The ε dependence of the reduced cross section as predicted from the polarization transfer results for G_E/G_M (red dashed line), and as measured in JLab E01-001 (circles). If the polarization transfer represents the true form factors, TPE yields more than half of the ε dependence at 2.64 GeV^2, and 85% at 4.1 GeV^2.

Analyses of the discrepancy of the Rosenbluth and polarization measurements that assume it is due primarily to missing corrections in the cross section measurements [11, 12, 15] indicate that the difference could be explained by an error in the ε dependence of the cross section of approximately 5–8% for $1 < Q^2 < 6$ GeV^2, which is consistent with other high-Q^2 analyses [7, 16]. The correction would have to be close enough to linear that it does not spoil the linearity expected from the Rosenbluth formula, as shown in Fig. 2, and detailed analyses have set significant limits on deviations from linearity over this Q^2 range [23].

One of the biggest problems with this sort of extraction is that it has to assume that the discrepancy is driven entirely by TPE contributions to the cross section measurements. Direct comparisons of positron-proton and electron-proton scattering can isolate the charge-odd terms associated with TPE. While recent comparisons yield results that are qualitatively consistent with modern TPE calculations, they do not reach the Q^2 region where there is a clear discrepancy, and so do not directly verify that the discrepancy is associated with TPE corrections.

We propose to measure the proton form factor ratio, G_E/G_M, using the Super-Rosenbluth (SR) technique separately for positron and electron scattering. The comparison of positron-proton cross sections and polarization transfer measurements (using electron beams) should show the opposite discrepancy as the electron cross section measurements for TPE, verifying that TPE contributions explain the observed discrepancy, and supporting the analyses that use the discrepancy to constrain TPE contributions and extract TPE-corrected form factors [16, 17]. We will also perform a measurements at the same Q^2 values with an electron beam. The difference between the electron and positron measurements is directly sensitive to the size and ε dependence of the TPE corrections, yielding twice the lever arm of the Rosenbluth-polarization comparisons while not relying on the assumption that the entire discrepancy is associated with TPE. Finally, the comparison of polarization results to the average of electron-proton and positron-proton scattering is a test of the charge-symmetric radiative correction procedures. Several works have examined the impact of updated or modified radiative correction procedures [24–26], which appear to explain up to $\sim$30% of the discrepancy [7, 26] based on more conventional radiative corrections [4, 27].

As discussed later in the proposal, the SR technique is extremely well suited for positrons, providing access to larger Q^2 values at low ε, where TPE contributions are large, and providing significant cancellation of systematic uncertainties between positron measurements at fixed Q^2 but different ε values. Electron and positron measurements are performed separately, and G_E/G_M is extracted from both with high precision. So while it does not make direct comparisons of the positron and electron cross sections at individual ε and Q^2 values, it also does not require frequent changes between electron and positron beams or a detailed understanding of their properties to minimize the systematic uncertainties in the direct cross section comparisons.

II. TWO-PHOTON EXCHANGE CONTRIBUTIONS

Electron scattering is generally treated in the one-photon exchange (OPE) approximation, after applying radiative corrections associated with Bremsstrahlung, loop, and vertex corrections [28, 29]. The IR-divergent terms associated with two-photon are included to cancel the divergence from soft photon emission, but the hard TPE contribution is generally neglected. In the 1950s and 1960s, several papers estimated the size of two-photon contributions to the unpolarized cross sections, using only the proton intermediate state [30], and including excited intermediate states [31–34]. These calculations predicted TPE effects consistent with the small differences between positron and electron scattering. Early measurements comparing positron and electron scattering, for which TPE contributions have the opposite sign, showed no significant contributions from TPE [35–41].

After the discrepancy between Rosenbluth separations and polarization measurements was observed and verified [8, 11, 42], it was shown [12] that TPE contributions, too small to be clearly observed in previous measurements [43], could resolve the discrepancy, as illustrated in Fig. 2. With even a small ε dependence, TPE corrections can have a significant impact on G_E/G_M at high Q^2, and can also lead to deviations from the linear dependence of the reduced cross section on ε required in the OPE. Since then, there have been many attempts to try and extract the TPE contributions from the observed discrepancy [7, 15, 17, 44], separate the TPE amplitudes [45, 46], constrain nonlinearities [23, 25], and to provide updated calculations of TPE at high Q^2 [13, 14, 25, 47–49]. Detailed reviews covering the experiments, analyses, and calculations can be found in Refs. [25, 50].

In the following sections, we present calculations of TPE contributions, direct measurements using the comparison of positron and electron scattering, and phenomenological estimates of the TPE contributions to the cross section.

A. Calculations of two-photon exchange corrections

Since the initial suggestions that TPE could resolve the proton form factors discrepancy [12, 13], there have been many attempts to provide improved TPE calculations, using a variety of approaches, e.g. hadronic vs. partonic degrees of freedom, dispersive approaches, etc..., and addressing a wide range of observables. We provide here a brief overview of some of these calculations, focused specifically on elastic electron-proton scattering. This provides a critical testing ground, where multiple observables can be measured over a wide range in Q^2, and these can be used to constrain calculations which can then be used to make predictions for other reactions or other observables.

Note that we focus entirely on calculations of the cross section, which are sensitive to the real part of the TPE amplitude, while other measurements, e.g. Born-forbidden normal asymmetries, are sensitive to the imaginary part of the TPE amplitude [25, 50]. So far, there are no calculations that fully explain the observed discrepancy in e-p scattering, and the calculations that do exist predict significantly different ε dependencies. Without additional data to constrain and improve these models, in particular at higher Q^2, we cannot rely on

them to identify potential TPE effects in other reactions. As such, we briefly summarize several approaches, but will focus on the observed discrepancy between Rosenbluth and polarization results when making projections for the Q^2 values relevant for this proposal.

Calculations by Blunden, Melnitchouk, and Tjon [25, 51] yield an ε dependence of approximately 3%, with small nonlinearities at low ε values and a weak Q^2 dependence. This calculation includes only the elastic portion of the two-photon correction; the box and crossed-box diagrams with the proton in the intermediate state, and neglect excited intermediate states. While this calculation largely resolves the form factor discrepancy for $Q^2 = 2$–3 GeV^2, it does not describe the discrepancy higher Q^2 values, and an additional phenomenological contribution had to be added to fully resolve the discrepancy in the analysis of [16].

Calculations by Chen, et al. [14] treat the two-photon exchange effect at the quark-parton level, using a generalized parton distribution to describe the emission and re-absorption of the partons by the nucleon. While this approach is not expected to be valid at low Q^2 or ε values, the calculations for higher Q^2 again show a significant ε dependence (and non-linearity) to the correction, with only a weak Q^2 dependence. This calculation provides roughly half of the TPE correction needed to explain the discrepancy at larger Q^2 values [25].

Calculations at the quark-parton level in the double logarithm approximation by Afanasev, et al. [52] yield a different form for the ε dependence, with nonlinearities appearing at large ε. However, it yields a very different nonlinearity from the calculation of Ref. [13]. In addition, it predicts only the ε and Q^2 dependence, but not the overall magnitude.

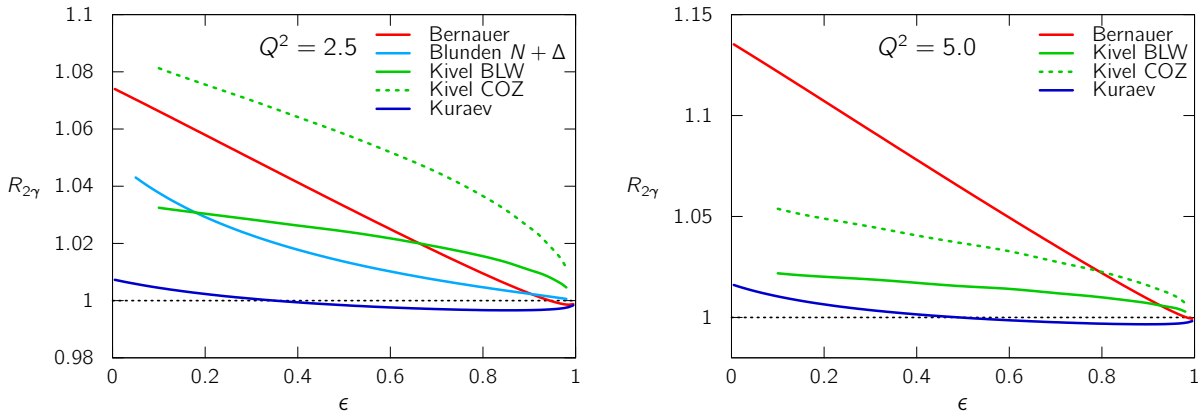

FIG. 3. The estimated two-photon exchange contribution to the positron-to-electron cross section ratio for a range of calculations and extractions at $Q^2 = 2.5$ and 5 GeV^2 [53]

B. Positron to electron comparisons

Two-photon exchange contributions to elastic electron–proton scattering can be observed in several different ways. The real part of the TPE amplitude modifies both the unpolarized cross section and the polarization transfer components used to extract G_E/G_M. The imaginary part of the amplitude leads to non-zero values for the Born-forbidden observables A_y

and P_N. These observables provide clean measurements of two-photon effects, but are not directly connected to the discrepancy in the form factors.

The main effect of TPE on the cross section comes from the interference between the one-photon and TPE amplitudes, $M_{1\gamma}$ and $M_{2\gamma}$:

$$\sigma(e^{\pm}p) = |M_{1\gamma} \pm M_{2\gamma}|^2 \approx M_{1\gamma}^2(1 \pm 2\mathrm{Re}(M_{2\gamma}/M_{1\gamma})). \quad (1)$$

Because the sign of the correction depends on the lepton charge, the ratio of positron to electron scattering, $R \equiv \sigma(e^+p)/\sigma(e^-p) \approx 1 + 4\mathrm{Re}(M_{2\gamma}/M_{1\gamma})$, is very sensitive to TPE effects. In the simplest approximation, one expects the two-photon amplitude to be suppressed by an additional factor of α, leading to a decrease of $2\alpha \approx 1.5\%$ in the electron cross section, and an increase of $4\alpha \approx 3\%$ in the ratio R.

In principle, the cleanest way to examine the effects of two-photon corrections in the unpolarized e–p cross section is to compare positron–proton and electron–proton scattering. Interference terms between one-photon and two-photon exchange have opposite signs for positron and electron scattering, and so yield a measurable difference. Early comparisons between e^+–p and e^-–p scattering [35], as well as μ^+–p and μ^-–p [54], were interpreted as showing that the two-photon corrections were extremely small (<1%). However, the low intensity of the positron (and muon) beams has made precise measurements nearly impossible for large Q^2 or small ε. There is some evidence of a charge-dependent term to the $e^{\pm}$–p elastic cross section at small values of ε [43], but the data at low ε is not very precise and is limited to Q^2 values well below the region of the observed discrepancy.

Measurements of the size of TPE through the e^+–p and e^-–p elastic cross section ratios were made at a number of facilities during the 1960s and 1970s. Due to the high precision necessary to see such an effect combined with the low intensity positron beam, a TPE effect generally consistent with unity was observed. With the discrepancy between Rosenbluth and polarization transfer, recent experiments have again sought to measure the effect by using this comparison of unpolarized electron-proton and positron-proton cross section. These experiments were performed at three independent facilities employing different experimental designs to measure the TPE contribution, $R_{2\gamma}$. They were performed at VEPP-3 in Novosibirisk, Russia [55, 56], Thomas Jefferson National Accelerator Facility using the CLAS spectrometer [57–59], and the DORIS electron/positron storage ring at DESY in Hamburg, Germany (Olympus) [60, 61]. The Olympus and VEPP-3 experiments switched between positron and electron beams and used mono-energetic beam energies while the CLAS experiment produced a mixed positron and electron beam and different beam energy settings. The Q^2 and ε range at which measurements were made were limited, largely below the higher Q^2 values where the pronounced discrepancy of G_E/G_M is observed or at low ε where the TPE effect is expected to be significant. Overall the data sets are in agreement and a global analysis including all three excludes a zero TPE effect at a 95% level, but most of the data is at $Q^2 < 1.5$ GeV^2, with a peak Q^2 value of just over 2 GeV^2. Comparison to various TPE calculations (see Figure 4) shows a systematic ε dependence that is reduced with the inclusion of TPE, but due to the limited coverage and limited data in the Q^2 region where a large form factor discrepancy is observed, a definitive conclusion of the source of

the discrepancy and importance of TPE for $Q^2 > 2$ GeV^2 remains.

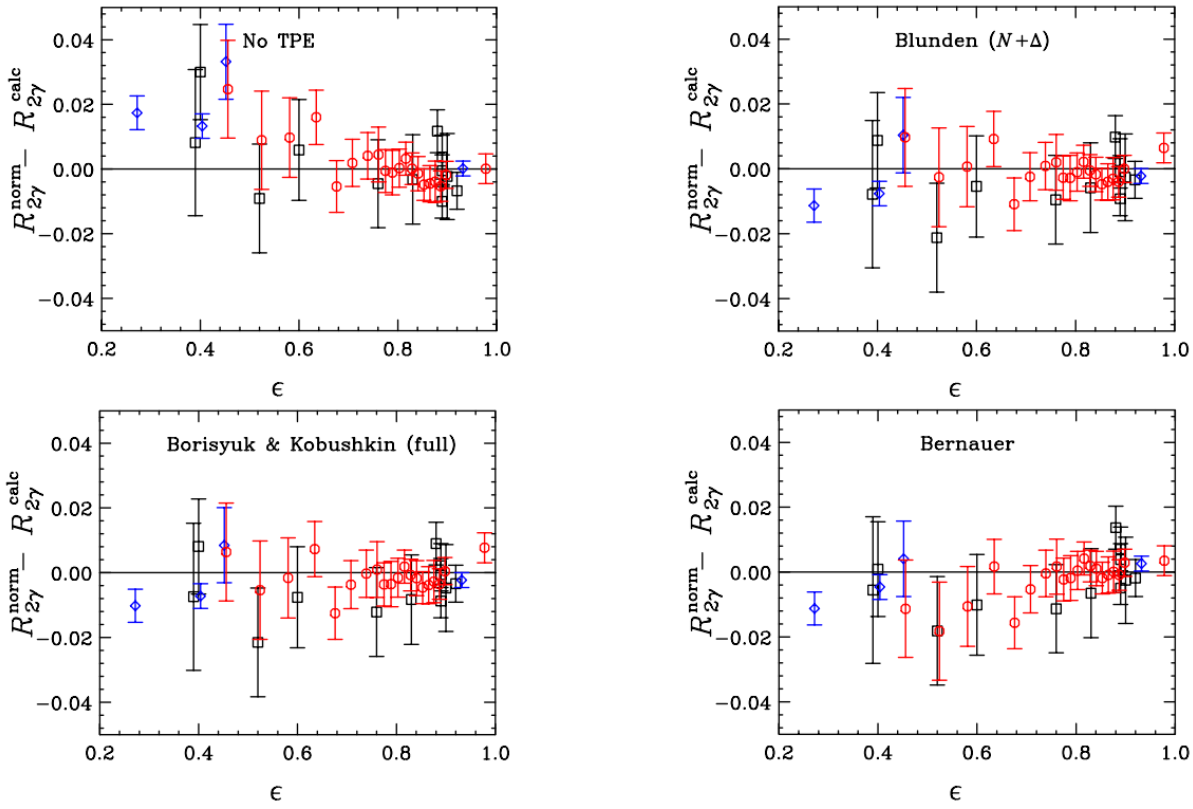

FIG. 4. Difference between the measure $R_{2\gamma}$ from e^+/e^- comparisons and different TPE calculations after allowing for renormalization of the different measurements [50]. The measurements are from VEPP-3 (blue diamonds), CLAS (black boxes), and OLYMPUS (red circles are the OLYMPUS). Figure reproduced from Ref. [50].

C. Phenomenological extractions of two-photon exchange corrections

As noted in the previous sections, calculations of the TPE contribution are generally in qualitative agreement, in that they all increase the observed slope and therefore G_E/G_M in Rosenbluth separations with electrons, but they differ in magnitude, especially at large Q^2 values, and show very different ε dependence. In addition, they are not large enough to completely explain the discrepancy at larger Q^2 values. As such, we will use phenomenological extractions of the TPE contributions to make predictions for what we should expect to see for a Rosenbluth separation with a positron beam under the assumption that TPE corrections to the cross section explain the entire discrepancy.

Early phenomenological extractions [11, 15–17, 44] generally assumed that the TPE contribution yielded a change in the slope of the reduced cross section vs ε, but maintained the linear dependence required in the one-photon exchange approximation. These yielded similar TPE corrections, requiring an ε dependence of ≈5-6% in the Q^2 region where a significant

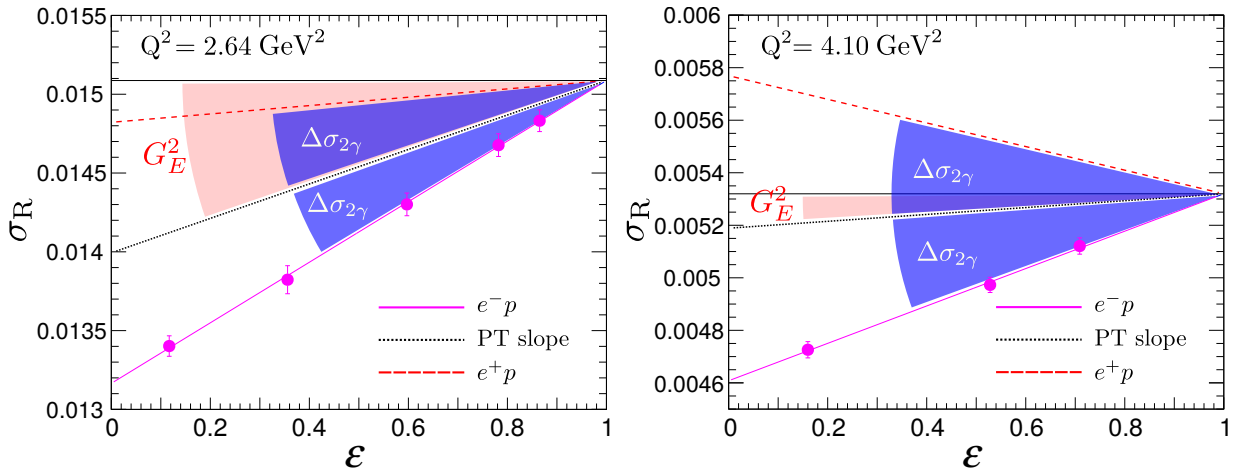

FIG. 5. The ε dependence of σ_R from the E01-001 e-p Super-Rosenbluth data at two Q^2 values [20] (purple points and linear fit) compared to the slope based on the recoil polarization data (black line). Assuming that the difference comes entirely from TPE, the red shaded region indicates the slope associated with the G_E contribution to the cross section, and the blue shaded region indicates the impact of TPE normalized to match the electron data at $\varepsilon = 1$, were TPE contributions go to zero [25]. Since TPE contributions change sign for positrons, the dotted red line shows the expected results for positron measurements, assuming a linear TPE contribution.

discrepancy was observed, as illustrated in Fig. 6. Later analyses made different assumptions about the ε dependence [62–64], with the assumption chosen for the ε dependence modifies both the ε and Q^2 dependence of the extracted TPE contributions.

Such extractions were recently extended to larger Q^2 values after the publication of new, high-Q^2 elastic scattering measurements from early 12 GeV running [7]. New measurements were combined with existing high-ε points to perform high-Q^2 Rosenbluth separations as well as a global fit up to $Q^2 \approx 15$ GeV^2, as shown in the right left of Figure 7. Based on the discrepancy between the global cross section fit and the polarization data, we can extract the TPE contribution assuming a linear contribution that is maximum at $\Delta_{2\gamma}$ at $\varepsilon = 0$, i.e. $\sigma_{TPE}/\sigma_{OPE} = 1 - \Delta_{2\gamma}(1-\varepsilon)$. Averaging the 7 high-$Q^2$ points shown in the right panel yields $\Delta_{2\gamma} = (4.2 \pm 2.0)\%$ for the TPE contribution above 6 GeV^2. However, for this analysis, updated radiative correction procedures [26] were applied to all of the cross sections used in the global analysis, and these updated corrections reduce the discrepancy somewhat compared to extractions made using Mo and Tsai based radiative corrections [4, 27]. The same analysis, performed with consistent radiative correction procedures, yields $\Delta_{2\gamma} = (6.6 \pm 2.1)\%$, consistent with previous analysis focusing on data for Q^2 from 2-5 GeV^2.

Note that the critical assumptions in these analysis are that TPE (1) fully explain the discrepancy, (2) modify the cross section via a linear ε-dependent contribution, and (3) do not modify the polarization transfer results significantly. If all of this is true, this sort of phenomenological extraction provides sufficient precision to extract the form factors reliably up to to at least $Q^2 \approx 6$ GeV^2 [16]. Comparisons of Super-Rosenbluth extractions of G_E/G_M will not only improve the precision of these extractions, they will directly address

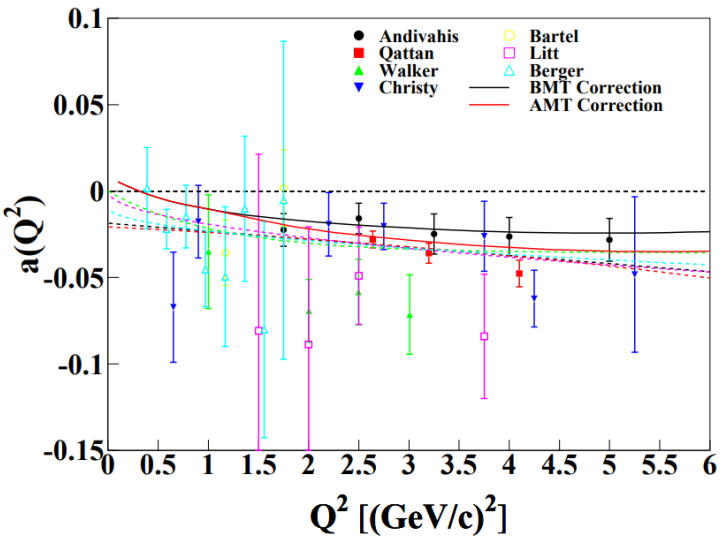

FIG. 6. TPE slope vs Q^2 from extraction of Ref. [44], along with slopes from hadronic calculations. The dotted lines are a variety of parameterizations used to fit the extracted $a(Q^2)$ values, where $\sigma_{TPE} = G_M^2(1 + (\varepsilon/\tau)R^2) + 2a(1-\varepsilon)G_M^2$, $R = \mu_p G_E/G_M$. Note that the peak TPE contribution at $\varepsilon = 0$ is equal to $2a$, and thus $a = 0.03$ corresponds to a 6% ε-dependent correction.

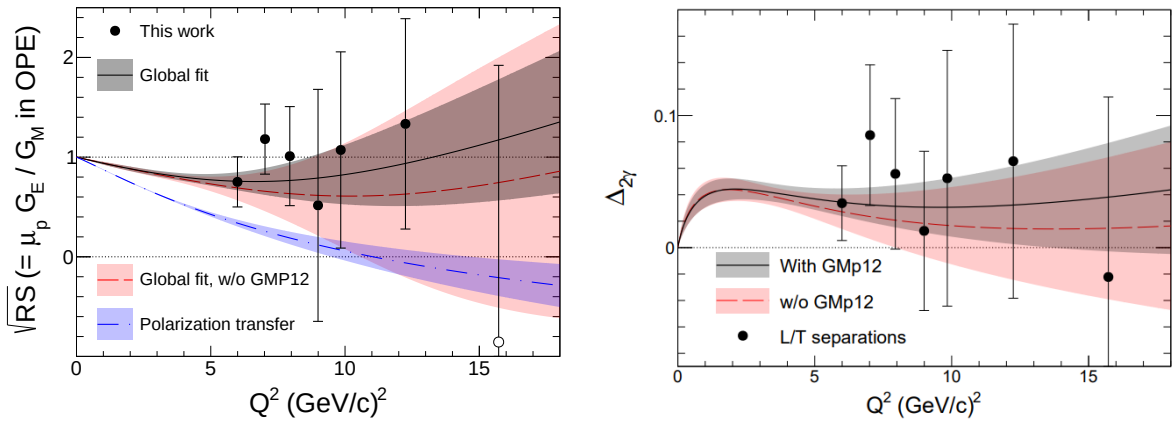

FIG. 7. (Left Panel) Rosenbluth separation results for $\sqrt{RS} = \mu_p G_E/G_M$ in the OPE. (Right Panel) $\Delta_2\gamma$ as a function of Q^2 from a global fit. Figures taken from [7]. The black solid (red dashed) curve shows the results from a global fit to the cross section data with (without) [7] data. The blue dot-dashed curve shows a fit to the polarization data. The shaded bands show the 68% confidence intervals of the respective fits.

the assumptions made in such analysis. Comparison of positron and electron SR extractions will isolate the charge-odd contributions associated with TPE, directly verifying for the first time whether or not TPE fully explains the discrepancy at large Q^2. The data will also provide improved constraints on potential non-linearity of the TPE exchange. Finally, by comparing electron and positron Rosenbluth separations, the sensitivity to TPE contributions is doubled compared to comparisons to polarization data, while being independent of

any potential TPE (or other systematic effects) in the polarization measurements.

III. EXPERIMENT

We propose to make a series of high-precision SR separation measurements to map out the ε and Q^2 dependence of the TPE contributions to the elastic e^-–p and e^+–p cross sections. In this experiment, we will use the spectrometers to detect the struck proton, rather than the scattered positron. The proton measurement allows a larger precision in extracting the ε dependence of the cross section leading to a cleaner G_E/G_M extraction, as it was shown by the E01-001 [20] experiment.

We will measure $\sigma(e^{\pm}p)$ using the same detectors and kinematic settings for $1 \lesssim Q^2 \lesssim 6$ GeV^2. We will focus on the ε dependence by extracting G_E/G_M with both electrons and positrons. Then, we will compare electron and positron results, making the result less sensitive to differences between electron and positron beams to account for potential long-term drifts in the detector response.

This proposal uses the benefits of the SR extractions by requiring multiple beam energies, this will allow to perform multiple separations at each Q^2. The measurements will improve the sensitivity to the ε dependence and possible non-linear contributions. In the following the experimental overview and the advantages of proton detection are summarized. The expected backgrounds are shown based in previous SR measurements (E01-001 experiment). Finally, the kinematics and beam time request is provided with an outline of the systematic contributions that are expected in the measurements.

A. Experimental overview

The experiment is proposed for Hall C using the standard HMS spectrometer and a hydrogen target. The 10 cm liquid hydrogen target will be viewed at a maximum angle of 53 degrees, so target length effects on the acceptance (after our solid angle and momentum acceptance cuts) will be negligible. The rate estimates are done with 2 μA and 20 μA for the porsitron and electron beams, respectively.

The beam energies required range from 0.65 to 11.0 GeV with a total of three different accelerator configurations. Time of flight and an Aerogel detector will be used for p/π separation. Solid angles will be restricted to 3.2 msr by software cuts to maintain 100% acceptance. Coincidence data will be taken for all setting with $\theta < 40^\circ$ to check our modeling of the background, the spectrometer resolution, and the radiative tail for the elastic peak.

B. Advantages of proton detection

The SR technique takes advantage of detecting protons in $\sigma(e^{\pm}p)$ elastic reactions. At fixed Q^2, the proton momentum is constant as shown in the top-left panel of Figure 8, so all momentum-dependent corrections cancel-out when examining the ε dependence. The cross section is much larger for proton detection at low ε, where cross section limits conventional Rosenbluth separations, and also has a much smaller ε dependence, reducing the impact of

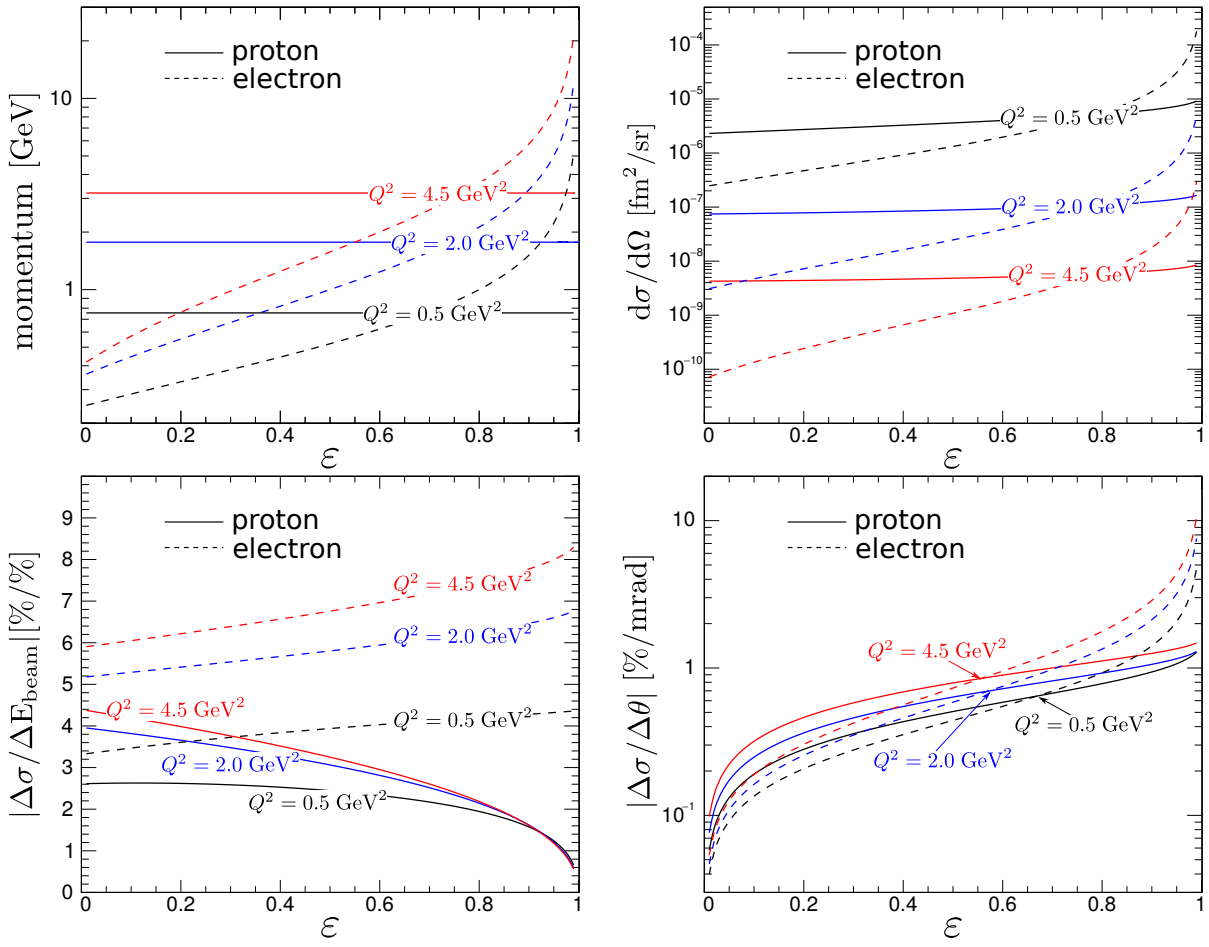

FIG. 8. Comparison of the ε dependence of various quantities for electron and proton detection for elastic e-p scattering. The top left panel shows the detected particle momentum, top right shows the inclusive detection cross section, and the bottom left (right) show the cross section sensitivity to beam energy (detected particle angle). Figure taken from Ref. [21].

rate-dependent effects. Proton detection also reduces the sensitivity to imperfect knowledge of the beam energy and angles, as the sensitivity to these quantities is generally smaller than for electron detection, especially at large ε, where these effects are the largest in electron detection, as shown in the bottom panels of Fig. 8. In addition, detection of the proton is insensitive to bremsstrahlung on the outgoing electron, which is strongly ε dependent due to the large range of scattered electron energy at fixed Q^2, as shown in Fig. 8. Because of this, the ε dependence of the radiative corrections is also smaller, making the Super-Rosenbluth extraction less sensitive to the details of the conventional radiative corrections. Figure 9 shows the ε dependence of the radiative correction for electron and proton detection at two Q^2 values.

The reduced sensitivity to the kinematics combined with the reduced ε dependence of the rate, momentum, and distribution of the elastically scattered proton allow for a much more precise extraction of G_E/G_M. While efficiencies or other rate or momentum-dependent corrections may still be significant and have a non-negligible uncertainty, they should be

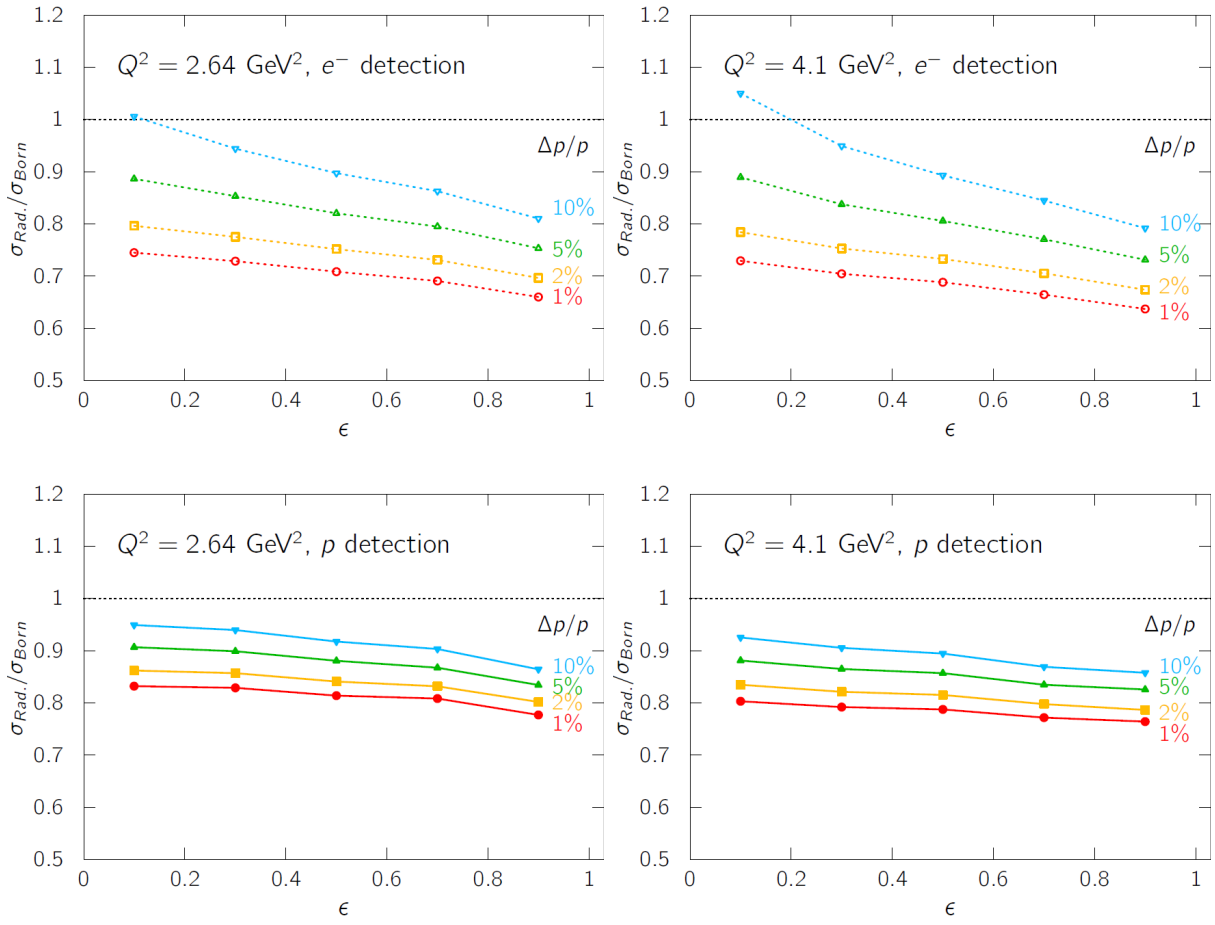

FIG. 9. Comparison of the ε dependence of the radiative correction for electron detection (top) and proton detection (bottom) for kinematics from two of the E01-001 Q^2 points. While the size of the radiative corrections are sometimes smaller and sometimes larger for proton detection, the ε dependence is significantly smaller for any value of the inelastic cutoff, $\Delta p/p$.

nearly constant for different ε settings at a fixed Q^2 values. Because G_E/G_M is related to the slope of the reduced cross section relative to its intercept, any common uncertainty cancels completely in the Rosenbluth extraction of G_E/G_M. Thus, momentum-dependent effects will have no impact, and rate dependent effects will have much less impact on the ε dependence. There is also a significantly smaller ε dependence to the bremsstrahlung correction, and thus a smaller correction that must be applied to the extraction of G_E/G_M. As demonstrated by E01-001 [20], and seen clearly in Fig. 1, this allows for a much higher precision in extracting G_E/G_M and examining the ε dependence of the cross section. While some corrections or uncertainties are larger when detecting the proton, e.g. associated with proton absorption in the spectrometer or the software-defined solid angle of the spectrometer, these yield uncertainty mainly in the *absolute* cross section, and have negligible effect on the extraction of the ε dependence.

C. Backgrounds

Figure 10 shows proton singles spectra as a function of $\delta\theta$ from E05-017, along with measured spectra from the target endcaps (green), and simulations of the e-p elastic (blue) and inelastic (magneta) protons from Compton scattering and pion production. $\delta\theta$ is the difference between the measured proton angle and the proton momentum calculated from the measured momentum assuming elastic scattering. The size of the background and simulated contributions is normalized against the measured data.

The contributions from the target endcaps are somewhat larger than in the case of positron detection, so we will take a larger fraction of the data on an aluminum 'dummy' target, and use a target that more closely matches the radiation length of the hydrogen target. For the spectrum at 2.64 GeV^2, the endcap subtraction varies between ∼15% at low ε ($-15 < \delta p < 15$ MeV) and ∼10% at high ε ($-25 < \delta p < 25$ MeV). With these δp cuts, we eliminate most of the non-endcap background contributions while staying away from the edges of the elastic peak. The ∼5% ε dependence in the background subtraction will be directly measured. Based in previous measurements, we expect the endcap contribution to better than 2%, yielding an uncertainty in the slope of 0.1%. Contributions to the non-linearity are even smaller because the size of the dummy subtraction varies approximately linearly with ε.

Photoproduction of neutral pions is the other significant source of high energy protons. Figure 10 shows the simulated spectrum for $Q^2 = 2.64$ GeV^2. For forward angle settings (small ε), this background is large but can be almost entirely eliminated with a reasonable cut on the elastic peak. At larger angles, the smaller resolution limits the precise subtraction of the backgroundd, however, the background can be reliably modeled. To verify our modeling of the background and the shape of the elastic peak, we will have coincidence runs at multiple kinematics which will allow us to separate the elastic events from the background processes and test our calculations of the line shapes.

Other source of background are of charged pions (up to a few percent for E01-001). Time of flight will efficiently remove pions for the low Q^2 data, and an Aerogel detector will be used to reject pions where the time of flight is not fully efficient. The pion contamination will be negligible after the particle identification cuts, while the inefficiency of the cuts for protons depends only on the proton momentum and thus does not introduce any significant uncertainty in the ε dependence.

D. Systematic uncertainties

Because of the high precision required for this measurement, we must ensure that we account for small corrections that are often neglected. In addition, we must separate out uncertainties which lead to a scale offset for all values at a given Q^2 from those which vary randomly from point-to-point, or those which vary linearly with ε. Table I summarizes the uncertainties for the extraction of the cross section and form factor ratio. These uncertainties are slightly better than those achieved in E01-001 [20], due mainly to improved statistics

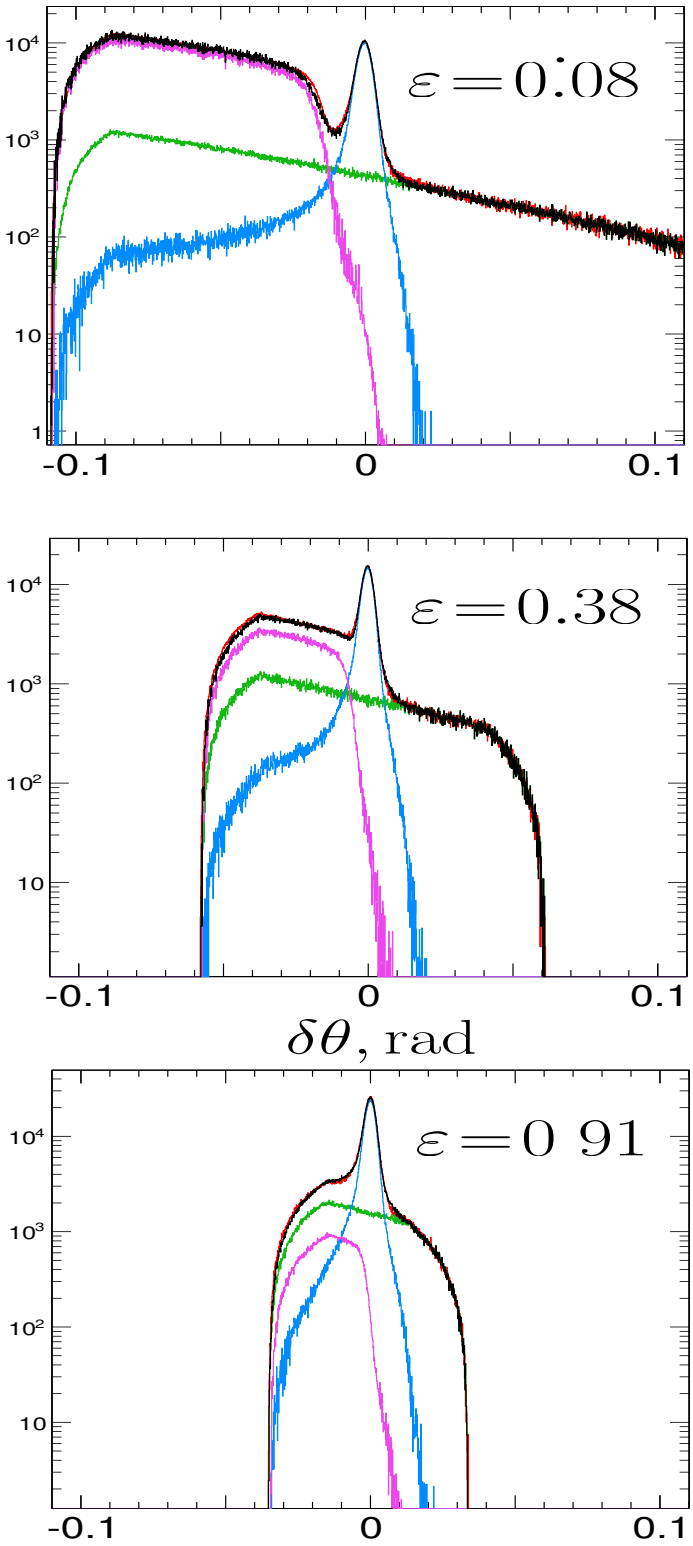

FIG. 10. Example of the Super-Rosenbluth data in the HMS for $Q^2 = 2.29$ GeV^2 for three ε settings. At very low ε, the inelastic background is large but can be normalized precisely and is well-separated from the elastic peak. At large ε, the background is not as well separated from the peak, but is more than an order of magnitude smaller.

Source	Size	$\delta\sigma/\sigma$ total	$\delta\sigma/\sigma$ G_E/G_M
Statistics	0.4%	0.4%	0.4%
Energy (fixed offset)	0.04%	0.2%	*0.1%
Energy (random)	0.04%	0.2%	0.2%
θ_p(fixed offset)	0.30 mr	0.2–0.5%	*0.3%
θ_p(random)	0.20 mr	0.1–0.3%	0.1–0.3%
Dead Time		0.1%	<0.1%
Dummy Subtraction		0.2–0.5%	*0.2%
Background Subtraction		0.1–1.0%	*0.3%
Radiative Corrections		1.2%	0.2%
			*0.2%
Luminosity		0.6%	0.2%
Proton absorption		1.0%	$\ll$0.1%
Acceptance		$\sim$2%	$\ll$0.1%
Efficiency		0.5%	$\ll$0.1%
Total		$\sim$2.9%	0.42–0.50%
			*0.52%

* Uncertainty given is on the slope rather than the individual cross sections

TABLE I. Projected uncertainties for the proposed cross section measurements.

and improved measurements of the backgrounds from endcap scattering. In addition, the extraction of G_E/G_M will benefit from the improved ε range of this proposal.

Computer dead time corrections are measured in the standard data acquisition system in Hall C with a very small associated uncertainty. Because of the relatively low rates in the experiment (below 30 kHz), the electronic dead time correction is at most 0.2%, and the ε dependence is a factor of two lower. A larger problem is the effect of multiple tracks in the chambers. While the tracking code does a good job of selecting the track that formed the trigger, there can be confusion in the tracking for overlapping events. The time window over which this could cause problems is 200-300 ns. For these measurements, the rates are low enough that we can reliably correct for these small (<1%) effects.

The uncertainty in the luminosity comes mainly from the measurement of the beam current and corrections for fluctuations in the target density. With the maximum expected beam current to 1-2 μA, all data will be taken at a fixed beam current. Thus, while the absolute uncertainty in the BCM calibration is about 0.5%, the fluctuation over time can be held to 0.2%. Compared to the common electron beam currents, which can reach 70 μA, the 2 μ positron beam current, along with the present target and raster, will result in density fluctuations due to heating that will be small.

At low Q^2, the elastic rate over the full solid angle varies from 0.2 kHz at low beam energy to 0.8 kHz at high beam energy. However, the inelastic backgrounds are larger at forward angles so the raw event rate should vary by less than a factor of two. The *maximum* raw

event rate will be roughly 1.1 kHz, leading to a small total correction for electronic deadtime ($\sim$0.1%) and multiple tracks ($\sim$0.7%), with an ε dependence that is less than half of this size. The uncertainties on these corrections will be less than 0.05%.

Significant systematic uncertainties can come from the uncertainty in the scattering kinematics, and so we will require beam energy measurements at each setting. The cross sections typically changes by 4–6% for a one percent change in beam energy, with little ε dependence. So an overall offset of 0.04% in the beam energy yields a scale uncertainty in the cross section of 0.2%, and an ε-dependent correction of 0.1%, very nearly linear in ε. The linearity measurement is much more sensitive to uncorrelated beam uncertainties. Assuming a point-to-point beam energy uncertainty of 0.04%, as obtained by E94-110 [6], the cross sections vary by about 0.2%.

The uncertainty in the angle of the scattered proton also breaks down into an overall offset (identical for both forward and backward angles) and an offset that can vary randomly as the spectrometer angle is changed. We expect to achieve an overall offset of 0.3 mr, somewhat larger than the 0.2 mr achieved in E94-110, due to the additional uncertainty associated with the software-defined solid angle. We may be able to do somewhat better since we can use the elastic scattering kinematics at each setting as a check on the angle offset. As seen in Fig. 8, a fixed offset yields a change in slope of 1% per mr, but maximum deviations from linearity of only 0.2% per mr. So a 0.3 mr offset yields a linear ε dependence of 0.3%, which contributes to the uncertainty in G_E/G_M, but yields deviations from linearity of $<$0.1%. For the linearity measurement, we are again more sensitive to angle offsets that vary randomly with changing scattering angles. E04-110 [6] achieved point-to-point uncertainties in the scattering angle of 0.2 mr. The sensitivity to the proton angle varies from 0.5–1.5% per mr, yielding uncertainties in the cross section of 0.1–0.3% (largest at large ε).

E. Kinematics

In order to map out the ε and Q^2 dependence of the TPE contributions, we will preform Rosenbluth separation at ten Q^2 points, providing precise extractions of G_E/G_M at Q^2=1.40, 1.69, 1.94, 2.4, 2.74 3.15, 3.81, 4.33 ,4.86 and 5.5 GeV^2. At each Q^2 we will measure the elastic positron-proton cross section at four ε points, spaced roughly uniformly up to the maximum possible value. To make these measurements, a series of beam energies, utilizing three linac settings, are required to cover the ε range. These settings were optimized to reduce the number of linac and beam energy changes required. Figure 11 shows the kinematics (Q^2 vs. ε) for elastic scattering at the proposed energies. The blue, purple, and black lines represent to the three linac settings. The four black dash-dotted lines correspond to the standard tune of 2200 MeV per pass (2.2, 4.4, 6.6, and 11.0 GeV respectively). The blue dashed and solid cyan lines correspond to linac settings of 650 and 730 MeV per pass respectively. These data will significantly improve the existing Rosenbluth extractions of $\mu_p G_E/G_M$, and allow us to use the discrepancy between Rosenbluth and polarization to make quantitative statements on the size of the two-photon amplitudes (Sec.II C).

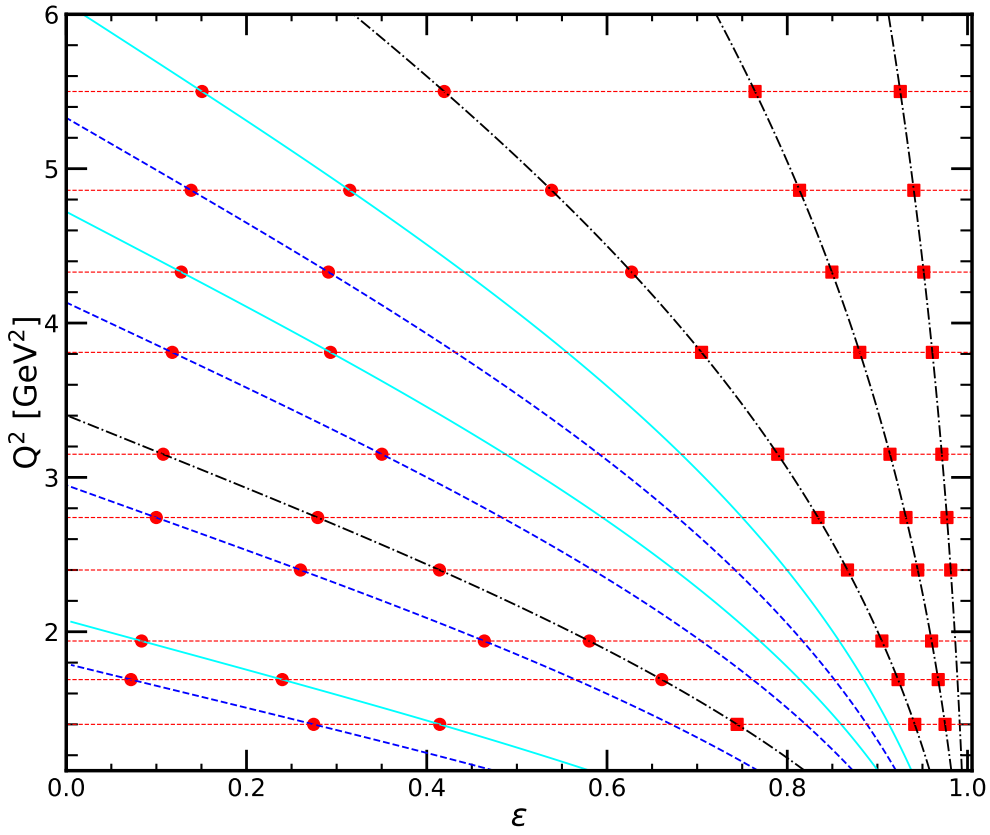

FIG. 11. The ε values that can be measured as a function of Q^2 for the available positron energies. The dashed red lines indicate the Q^2 values where we will make precise measurements of G_E/G_M. The red circles and squares indicate the points where measurements will be taken, with the red squares highlighting kinematics at which coincidence data can be taken. The minimum ε value is determined by the assumed minimum scattering angle of 11 degrees.

F. Beam time request

Data taking for the points shown in Fig. 11 is summarized in Table II. We request a total of 13 PAC days, including the main data taking, calibration and checkout runs, and overhead for beam energy and changes.

While the main data taking uses the hydrogen target, data taken on an aluminum 'dummy' target will be used to subtract the contributions from the target endcaps. We will also take runs at at different beam currents to verify our measurement of the target heating effects, dead time, and other rate-dependent effects in the spectrometers. Data will be taken with a thin carbon target at all kinematics as a check on the target position and beam offsets. Finally, coincidence data will be taken at some settings as a check of the scattering kinematics and as a measure of proton detection efficiency and absorption, even though these corrections cancel in the ε dependence. We can also use the coincidence data to examine the elastic proton spectrum without the backgrounds, allowing us to check the agreement between the data and the simulated elastic (and background) spectra. These

	positron time[hrs]		electron time[hrs]
Q^2=1.40	5 × 1.0 hrs	5	5
Q^2=1.69	5 × 1.0 hrs	5	5
Q^2=1.94	5 × 1.2 hrs	6	5
Q^2=2.4	5 × 2.0 hrs	10	5
Q^2=2.74	5 × 3.2 hrs	16	5
Q^2=3.15	5 × 5.5 hrs	28	6
Q^2=3.81	5 × 11 hrs	55	11
Q^2=4.33	5 × 19 hrs	95	19
Q^2=4.86 (0.5% statistics)	5 × 22 hrs	110	22
Q^2=5.5 (0.6% statistics)	4 × 24 hrs	96	25
High stat. coincidence runs	8 × 4 hrs	32	32
Dummy target data	(20% of LH2 data)	92	16
Total production		**550**	**156**
Target boiling studies		4	4
BCM calibrations		8	8
Checkout/calibration		12	12
Beam energy measurements	12 × 1 hr	12	12
linac changes	3 × 12 hrs	36	36
pass changes	9 × 6 hrs	56	56
kinematics changes	40 × 0.5 hrs	20	20
Total overhead/calibration		**148**	**148**
Total		**698 (29 days)**	**304 (13 days)**

TABLE II. Beam time request for the positron and electron measurements. Electron running time is at higher current, but takes somewhat higher statistics to provide additional resolution and background studies, as the time is dominated by overhead.

runs will be taken for every setting where the SHMS can measure the scattered electrons ($\theta_e < 40°$).

IV. PROJECTED RESULTS FOR THE PROPOSED MEASUREMENTS

Figure 11 shows the kinematics of the proposed measurements, with circles indicating the proton-only kinematics, and squares indicating kinematics where we will also take coincidence events. Table I summarizes the systematic uncertainties for the cross section measurements. Separate entries are given for the total uncertainty in the absolute cross sections, the uncertainties that enter into the extraction of G_E/G_M (neglecting ε-independent uncertainties), and the uncertainties that enter into the linearity tests (neglecting the portions of the systematic uncertainties that vary *linearly* with ε).

Fig. 5 illustrates the expectation for the ε dependence of both electron and positron measurements at two Q^2 values. The uncertainties on the electron data come from E01-001 [20], and we expect comparable uncertainties for both the positron and electron Super-Rosenbluth measurements proposed here. Note that for larger Q^2 values, the contribution from G_E, as determined from the polarization data, is very small, and even for $Q^2 \approx 2$ GeV^2 and above, the uncertainty on G_E yields a very small uncertainty on the expected Rosenbluth Slope (RS) in the OPE approximation, as illustrated in Fig. **??**.

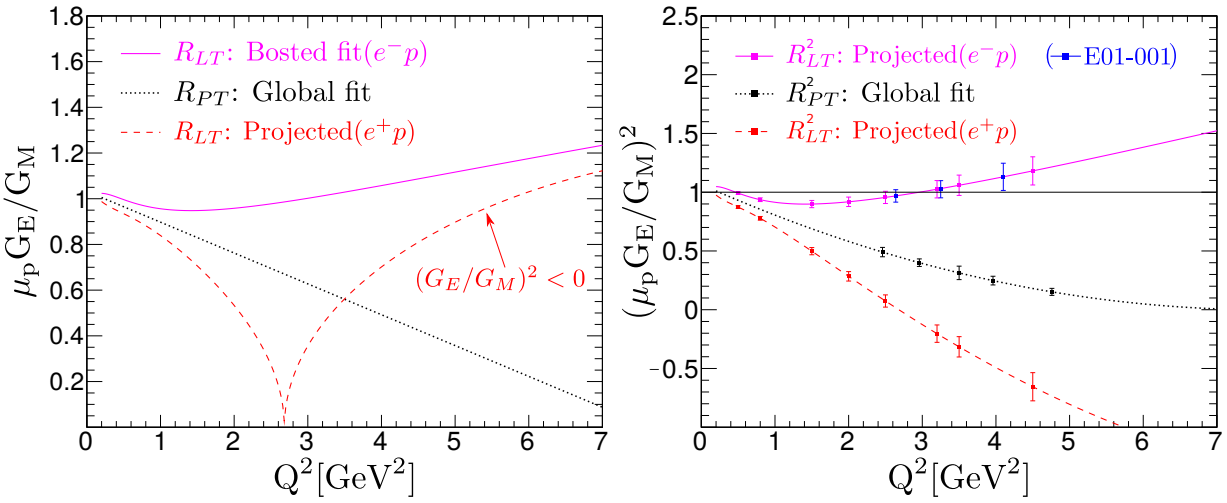

FIG. 12. [Left] Form factor ratio as a function of Q^2 for electron scattering [5] (magenta line), the polarization data [22] (black line), and the projected results for positron scattering assuming that the TPE contribution explains the full difference between the electron Rosenbluth extractions and recoil polarization. Note that for $Q^2 > 2.7$ GeV^2, $(G_E/G_M)^2 < 0$ and the curve represents the square rood of the absolute value of $(G_E/G_M)^2$ [Right] Same, but showing the form factor ratio squared, which directly corresponds to the observed slope in the Rosenbluth separation.

This can be converted to a prediction for the form factor ratio $\mu_p G_E/G_M$ as a function of Q^2 for positron and electron Rosenbluth separations and for polarization measurements. The right hand of Figure 12 plot shows $(\mu_p G_E/G_M)^2$, which corresponds directly to the observed slope in the Rosenbluth separations. Note that based on the parameterizations used here, this slope becomes negative above $Q^2 \approx 2.7$ GeV^2. Since this corresponds to an imaginary value for $\mu_p G_E/G_M$, the left plot takes the absolute value of the slope. As such, we show projected uncertainties only for the right hand plot.

As noted earlier, combining the electron and positron Rosenbluth results yields a precise extraction of G_E/G_M with no TPE contributions, and comparisons of this to the polarization extraction provides a test of the conventional charge-even radiative correction procedures. This will allow a test of older RC procedures and newer formalisms.

Finally the contribution of G_E to the reduced cross section is small, with even smaller uncertainties, for $Q^2 \approx 3-4$ GeV^2 and above (see Fig. 5). Therefore, the ϵ dependence will provide a precise measurement of measure of not only the size of the TPE contribution, but the ε dependence as well, negligible uncertainty from the uncertainty in the knowledge of the G_E contribution.

In conclusion, with we provide the following:

- First direct verification of the idea that TPE explain the form factor discrepancy for $1.4 < Q^2 < 5.5$ GeV^2
- Test of the conventional radiative correction procedures
- Confirming TPE as the source of the discrepancy will confirm previous phenomenological extractions and, with our data, provide improved constraints on size of the TPE contributions.
- Provide improved constraints on non-linearity in the TPE contributions, free from the effect of potential imperfections in the conventional radiative corrections.

The proposed measurements here are complementary to direct $\sigma(e^+)/\sigma(e^-)$ measurements. While this proposal does not provide direct measurements of $\sigma(e^+)/\sigma(e^-)$ for individual ε, Q^2 points, it allows for precise comparisons of the Rosenbluth Slope for positron and electron scattering, while providing several advantages over direct cross section ratios.

- Significant cancellation of experimental systematic effects between positron measurements at fixed Q^2 but different ε values. As such, positron and electron measurements can be performed separately, and do not rely on conditions being identical for positron and electron running
- High precision on ε dependence allows for precise measurement of ε dependence including potential non-linear contributions
- The cross section for small-ε scattering, where TPE are expected to be the largest, is larger by up to an order of magnitude with proton detection vs electron detection.
- Smaller ε dependence in the RC for proton detection compared to electron detection.

[1] J. J. Kelly, Nucleon charge and magnetization densities from sachs form factors, Phys. Rev. C **66**, 065203 (2002).
[2] S. Venkat, J. Arrington, G. A. Miller, and X. Zhan, Realistic Transverse Images of the Proton Charge and Magnetic Densities, Phys. Rev. C **83**, 015203 (2011).
[3] G. A. Miller, Defining the proton radius: A unified treatment, Phys. Rev. C **99**, 035202 (2019).
[4] R. C. Walker *et al.*, Phys. Rev. D **49**, 5671 (1994).
[5] P. E. Bosted, Phys. Rev. C **51**, 409 (1994).
[6] M. E. Christy *et al.*, Measurements of electron proton elastic cross sections for 0.4 $(\mathrm{GeV/c})^2 < Q^2 < 5.5$ $(\mathrm{GeV/c})^2$, Phys. Rev. C **70**, 015206 (2004).
[7] M. E. Christy *et al.*, Form Factors and Two-Photon Exchange in High-Energy Elastic Electron-Proton Scattering, Phys. Rev. Lett. **128**, 102002 (2022).
[8] M. K. Jones *et al.*, Phys. Rev. Lett. **84**, 1398 (2000).
[9] A. J. R. Puckett *et al.*, Final Analysis of Proton Form Factor Ratio Data at $Q^2 = 4.0$, 4.8 and 5.6 GeV^2, Phys. Rev. C **85**, 045203 (2012).
[10] A. J. R. Puckett *et al.*, Recoil Polarization Measurements of the Proton Electromagnetic Form Factor Ratio to $Q^2 = 8.5$ GeV^2, Phys. Rev. Lett. **104**, 242301 (2010).
[11] J. Arrington, How well do we know the electromagnetic form factors of the proton?, Phys. Rev. C **68**, 034325 (2003).
[12] P. A. M. Guichon and M. Vanderhaeghen, How to reconcile the rosenbluth and the polarization transfer method in the measurement of the proton form factors, Phys. Rev. Lett. **91**, 142303 (2003).
[13] P. G. Blunden, W. Melnitchouk, and J. A. Tjon, Two-photon exchange and elastic electron proton scattering, Phys. Rev. Lett. **91**, 142304 (2003).
[14] Y. C. Chen, A. Afanasev, S. J. Brodsky, C. E. Carlson, and M. Vanderhaeghen, Partonic calculation of the two-photon exchange contribution to elastic electron proton scattering at large momentum transfer, Phys. Rev. Lett. **93**, 122301 (2004).
[15] J. Arrington, Implications of the discrepancy between proton form factor measurements, Phys. Rev. C **69**, 022201(R) (2004).
[16] J. Arrington, W. Melnitchouk, and J. A. Tjon, Global analysis of proton elastic form factor data with two-photon exchange corrections, Phys. Rev. **C76**, 035205 (2007).
[17] J. C. Bernauer *et al.* (A1), Electric and magnetic form factors of the proton, Phys. Rev. C **90**, 015206 (2014).
[18] X. Zhan *et al.*, High-Precision Measurement of the Proton Elastic Form Factor Ratio $\mu_p G_E/G_M$ at low Q^2, Phys. Lett. B **705**, 59 (2011).
[19] G. Ron *et al.* (Jefferson Lab Hall A), Low Q^2 measurements of the proton form factor ratio $\mu_p G_E/G_M$, Phys. Rev. C **84**, 055204 (2011).
[20] I. A. Qattan *et al.*, Precision Rosenbluth measurement of the proton elastic form-factors, Phys. Rev. Lett. **94**, 142301 (2005).
[21] J. R. Arrington and M. Yurov, A measurement of two-photon exchange in Super-Rosenbluth separations with positron beams, Eur. Phys. J. A **57**, 319 (2021).
[22] O. Gayou *et al.*, Phys. Rev. Lett. **88**, 092301 (2002).
[23] V. Tvaskis, J. Arrington, M. E. Christy, R. Ent, C. E. Keppel, Y. Liang, and G. Vittorini, Experimental constraints on non-linearities induced by two-photon effects in elastic and inelastic

Rosenbluth separations, Phys. Rev. C **73**, 025206 (2006).
[24] L. C. Maximon and J. A. Tjon, Radiative corrections to electron proton scattering, Phys. Rev. C **62**, 054320 (2000).
[25] J. Arrington, P. G. Blunden, and W. Melnitchouk, Review of two-photon exchange in electron scattering, Prog. Part. Nucl. Phys. **66**, 782 (2011).
[26] A. V. Gramolin and D. M. Nikolenko, Reanalysis of Rosenbluth measurements of the proton form factors, Phys. Rev. C **93**, 055201 (2016).
[27] R. Ent *et al.*, Radiative corrections for (e,e'p) reactions at GeV energies, Phys. Rev. C **64**, 054610 (2001).
[28] L. W. Mo and Y.-S. Tsai, Radiative corrections to elastic and inelastic e p and mu p scattering, Rev. Mod. Phys. **41**, 205 (1969).
[29] Y. S. Tsai, *SLAC-PUB-848*, Tech. Rep. (SLAC Report, 1971).
[30] R. R. Lewis, Phys. Rev. **102**, 537 (1956).
[31] S. D. Drell and M. Ruderman, Phys. Rev. **106**, 561 (1957).
[32] S. D. Drell and S. Fubini, Phys. Rev. **113**, 741 (1959).
[33] N. R. Werthammer and M. A. Ruderman, Phys. Rev. **123**, 1005 (1961).
[34] G. K. Greenhut, Phys. Rev. **184**, 1860 (1969).
[35] J. Mar *et al.*, A comparison of electron-proton and positron-proton elastic scattering a four momentum transfers up to 5.0 GeV^2, Phys. Rev. Lett. **21**, 482 (1968).
[36] R. L. Anderson, B. Borgia, G. L. Cassiday, J. W. DeWire, A. S. Ito, and E. C. Loh, Positron-proton elastic scattering at 800 and 1200 mev, Phys. Rev. **166**, 1336 (1968).
[37] B. Bouquet, D. Benaksas, B. Grossetete, B. Jean-Marie, G. Parrour, J. P. Poux, and R. Tchapoutian, Backward scattering of positrons and electrons on protons, Phys. Lett. B **26**, 178 (1968).
[38] W. Bartel, B. Dudelzak, H. Krehbiel, J. M. McElroy, R. J. Morrison, W. Schmidt, V. Walther, and G. Weber, Phys. Lett. B **25**, 242 (1967).
[39] R. L. Anderson, B. Borgia, G. L. Cassiday, J. W. DeWire, A. S. Ito, and E. C. Loh, Scattering of positrons and electrons from protons, Phys. Rev. Lett. **17**, 407 (1966).
[40] A. Browman, F. Liu, and C. Schaerf, Positron-proton scattering, Phys. Rev. **139**, B1079 (1965).
[41] D. Yount and J. Pine, Scattering of high-energy positrons from protons, Phys. Rev. **128**, 1842 (1962).
[42] O. Gayou *et al.*, Phys. Rev. C **64**, 038202 (2001).
[43] J. Arrington, Evidence for two-photon exchange contributions in electron-proton and positron-proton elastic scattering, Phys. Rev. C **69**, 032201(R) (2004).
[44] I. A. Qattan, A. Alsaad, and J. Arrington, Reexamination of phenomenological two-photon exchange corrections to the proton form factors and $e^{+-}p$ scattering, Phys. Rev. C **84**, 054317 (2011).
[45] J. Arrington, Extraction of two-photon contributions to the proton form factors, Phys. Rev. C **71**, 015202 (2005).
[46] J. Guttmann, N. Kivel, M. Meziane, and M. Vanderhaeghen, Determination of two-photon exchange amplitudes from elastic electron-proton scattering data, Eur. Phys. J. A **47**, 77 (2011).
[47] N. Kivel and M. Vanderhaeghen, Two-photon exchange in elastic electron-proton scattering: QCD factorization approach, Phys. Rev. Lett. **103**, 092004 (2009).
[48] D. Borisyuk and A. Kobushkin, Two-photon exchange amplitude with πN intermediate states:

Spin-1/2 and spin-3/2 channels, Phys. Rev. C **92**, 035204 (2015).
[49] P. G. Blunden and W. Melnitchouk, Dispersive approach to two-photon exchange in elastic electron-proton scattering, Phys. Rev. C **95**, 065209 (2017).
[50] A. Afanasev, P. G. Blunden, D. Hasell, and B. A. Raue, Two-photon exchange in elastic electron–proton scattering, Prog. Part. Nucl. Phys. **95**, 245 (2017).
[51] P. G. Blunden, W. Melnitchouk, and J. A. Tjon, Two-photon exchange in elastic electron-nucleon scattering, Phys. Rev. C **72**, 034612 (2005).
[52] A. Afanasev, S. Brodsky, and C. Carlson, (2003), presented at the Oct. 2003 DNP Meeting.
[53] Q. Stefan and A. Schmidt, Publication in preparation.
[54] L. Camilleri *et al.*, High-energy muon-proton scattering - one-photon exchange tests, Phys. Rev. Lett. **23**, 149 (1969).
[55] J. Arrington, V. F. Dmitriev, R. J. Holt, D. M. Nikolenko, I. A. Rachek, Y. V. Shestakov, V. N. Stibunov, D. K. Toporkov, and H. de Vries, Two-photon exchange and elastic scattering of electrons/positrons on the proton. (Proposal for an experiment at VEPP-3), in *11th International Seminar on Electromagnetic Interactions of Nuclei* (2007) p. 104, arXiv:nucl-ex/0408020.
[56] I. A. Rachek *et al.*, Measurement of the two-photon exchange contribution to the elastic $e^{\pm}p$ scattering cross sections at the VEPP-3 storage ring, Phys. Rev. Lett. **114**, 062005 (2015).
[57] M. Moteabbed *et al.* (CLAS), Demonstration of a novel technique to measure two-photon exchange effects in elastic $e^{\pm}p$ scattering, Phys. Rev. C **88**, 025210 (2013).
[58] D. Adikaram *et al.* (CLAS), Towards a resolution of the proton form factor problem: new electron and positron scattering data, Phys. Rev. Lett. **114**, 062003 (2015).
[59] D. Rimal *et al.* (CLAS), Measurement of two-photon exchange effect by comparing elastic $e^{\pm}p$ cross sections, Phys. Rev. C **95**, 065201 (2017).
[60] R. Milner *et al.* (OLYMPUS), The OLYMPUS Experiment, Nucl. Instrum. Meth. A **741**, 1 (2011).
[61] B. S. Henderson *et al.* (OLYMPUS), Hard Two-Photon Contribution to Elastic Lepton-Proton Scattering: Determined by the OLYMPUS Experiment, Phys. Rev. Lett. **118**, 092501 (2017).
[62] Y.-C. Chen, C.-W. Kao, and S.-N. Yang, Is there model-independent evidence of the two-photon-exchange effect in the electron-proton elastic scattering cross-section?, Phys. Lett. B **652**, 269 (2007).
[63] W. M. Alberico, S. M. Bilenky, C. Giunti, and K. M. Graczyk, Electromagnetic form factors of the nucleon: New Fit and analysis of uncertainties, Phys. Rev. C **79**, 065204 (2009).
[64] I. A. Qattan, New extraction of the elastic scattering cross-section ratio Re+e− at high Q2, Phys. Rev. C **107**, 045202 (2023).